arXiv:cond-mat/9712281v1 [cond-mat.str-el] 23 Dec 1997

Local Magnetic Impurities in the 2D Quantum Heisenberg Antiferromagnet

V.N. Kotov, J. Oitmaa, and O. Sushkov

School of Physics, University of New South Wales, Sydney 2052, Australia

The two-dimensional (2D) quantum Heisenberg antiferromagnet at zero temperature, with locally frustrating magnetic defects, is studied. We consider two types of defects - an isolated ferromagnetic bond (FMB) and a quantum impurity spin, coupled symmetrically to the two sub-lattices. A technique is developed to study strong defect-environment interaction. In the case of a FMB we find that, contrary to the previous linear spin-wave result, the local magnetization stays finite even for strong frustration. For an antiferromagnetic coupling of a quantum impurity spin with its environment, we find a local change in the ground state. All our calculations are compared with numerical results from exact diagonalization.

PACS numbers: 75.10.Jm, 75.30.Hx, 75.50.Ee

I. INTRODUCTION

The two-dimensional quantum Heisenberg antiferromagnet (HAFM) has attracted a lot of attention in the last several years, mainly because of its relevance to the physics of the high-T_c materials[1]. At zero hole doping, these compounds form planes of localized Cu spins and their physics is well described by the spin-1/2 square lattice HAFM. There is strong numerical evidence that this system has long-range order (LRO) in its ground state at $T = 0$. Due to quantum fluctuations, the staggered magnetic moment was found to be reduced to about 61% of the classical value[1]. Doping with excess oxygen, which is crucial for superconductivity, creates spin-1/2 holes on the oxygen sites, located in between the Cu sites. The holes interact magnetically with their Cu neighbors. This interaction leads to frustration of the Cu spins and ultimately to destruction of magnetic LRO, above a critical dopant concentration.

One way to describe the doping process is via an effective one-band model, like, e.g. the $t - J$ model[2], in which the holes hop in the antiferromagnetic (AFM) environment.

However, the extreme limit of static holes, which frustrate the AFM order only locally, is also believed to have relevance. The basic idea, put forward by Aharony *et al.*[3], is that a hole, interacting with its two neighbors creates an effective *ferromagnetic* interaction between them. The magnetic properties then are described by a HAFM with a given concentration of such ferromagnetic bonds (FMB). As a start, it is important to understand the effect that one isolated FMB has on the AFM environment. This problem was studied by Lee and Schlottmann[4] and Aristov and Maleev[5] in the linear spin-wave approximation (LSWA). They found that the magnetization of the two spins, connected by the bond decreases dramatically as the strength of the bond increases, and noted an instability that occurs in the theory at the "classical" transition point (the point where a local triplet formation is favorable without taking quantum fluctuation into account). There have been several extensions of this work, taking into account finite temperature and finite concentration of bonds[6,7]. One can also treat the frustration effects more realistically, by considering a model of frustration, in which

a static hole interacts with its two neighbor spins. Oitmaa, Betts, and Aydin[8] studied this model numerically, via an exact diagonalization on small clusters, and found a discontinuous local phase transition for an antiferromagnetic hole-neighbor interaction, whereas no change in the ground state occurred for a ferromagnetic coupling. A similar model was studied by Clarke, Giamarchi, and Shraiman[9] in one dimension via bosonization.

In the present work we study the two models with local frustration, mentioned above - an isolated FMB in the 2D HAFM, and a quantum defect spin, coupled symmetrically to the two sub-lattices. Our motivation is twofold. First, the basic works on the FMB problem[4,5] use the LSWA, which is only valid for small FMB strength. In the original frustration model however, Aharony *et al.*[3] concluded that the induced FMB coupling should be large. Thus, it is important to study the model for strong coupling, and, along the way, assess the region of validity of LSWA. Second, the two-dimensional spin defect model, which provides a realistic frustration mechanism, has not been studied analytically, as far as we know. The present work, thus, extends the previous work of Oitmaa, Betts, and Aydin[8] on this problem.

Our analytical approach is specifically designed to treat the strong coupling regime. The main idea is that since the perturbations are local, one should first solve the defect problem separately, and then take into account the defect-AFM environment interaction. For the FMB problem this amounts to considering the two-body Green's function of the two spins, connected by the bond. Analogously, for the spin defect problem, we introduce a three-body Green's function (of the spin defect and its two neighbors). All our analytical results are compared with numerical simulations, based on exact diagonalization on small clusters. A short account of the main results of this work appeared previously in Ref.[10]. The rest of the paper is organized as follows. Sec.II describes the basic idea behind our theoretical approach and, as a first application, we consider the HAFM with no defects. In Sec.III we present our analytical, as well as numerical solution of the FMB problem. Sec.IV deals with the spin defect problem from the same perspective. Our conclusions are summarized in Sec.V.

II. METHOD DESCRIPTION.

Consider the two-dimensional spin-1/2 Heisenberg model on a square lattice at zero temperature:

$$H_J = J \sum_{<i,j>} \vec{S}_i . \vec{S}_j . \tag{1}$$

The summation is over nearest neighbors only, and $J > 0$. We set $J = 1$ from now on. It is known[1] that there is LRO in the ground state of H_J and the staggered magnetic moment $m \equiv < S_i^z > = 0.303$.

Now assume we introduce additional interactions (of typical strength K) between two nearest neighbor spins. Let us call such a configuration a spin defect. We have in mind, for example, a FMB, connecting two of the spins. Since such a defect is local, it does not affect significantly the LRO far away from it. Therefore, in order to treat the strong coupling regime ($K \sim J$), one must first take into account the interaction between the spins in the defect and then treat the defect-AFM environment interaction.

As a simple illustration of the above idea consider the HAFM (1) without any additional interactions. Let a "defect" consist of only one spin $\vec{S}_1$, and separate (1) into an AFM background (spin-wave) Hamiltonian and a defect-neighbor interaction:

$$H = H_{sw} + S_1^z \sum_{i=2}^{5} S_i^z + \left\{ \frac{1}{2} S_1^+ \sum_{i=2}^{5} S_i^- + \text{ h.c.} \right\}, \tag{2}$$

$$H_{sw} = \sum_{\mathbf{k}} \varepsilon_{\mathbf{k}} (\alpha_{\mathbf{k}}^\dagger \alpha_{\mathbf{k}} + \beta_{\mathbf{k}}^\dagger \beta_{\mathbf{k}}). \tag{3}$$

Here is $\beta_{\mathbf{k}}$ and $\alpha_{\mathbf{k}}$ are the usual spin-wave operators with dispersion[1]:

$$\varepsilon_{\mathbf{k}} = 2\sqrt{1 - \gamma_{\mathbf{k}}^2}, \ \gamma_{\mathbf{k}} = \frac{1}{2}(\cos(k_x) + \cos(k_y)). \tag{4}$$

Next, the Ising part of the interaction in (2) is taken into account in the mean-field approximation, i.e. we replace: $\sum_{i=2}^{5} S_i^z \to 4m$. For the spin $\vec{S}_1$ it is convenient to use the fermion representation:

$$S_1^+ = \Psi_\uparrow^\dagger \Psi_\downarrow, \quad S_1^z = \frac{1}{2}(\Psi_\uparrow^\dagger \Psi_\uparrow - \Psi_\downarrow^\dagger \Psi_\downarrow), \tag{5}$$

where $\Psi_\uparrow^\dagger$ and $\Psi_\downarrow^\dagger$ create (acting on their common vacuum) a S_1^z component $1/2$ and $-1/2$ respectively. In order for the two fermions to represent a spin-1/2 operator, they have to satisfy the constraint: $\Psi_\uparrow^\dagger \Psi_\uparrow + \Psi_\downarrow^\dagger \Psi_\downarrow = 1$, i.e. the physical states have only one fermion. In this representation the Hamiltonian becomes:

$$H = H_{sw} + H_0 + H_{int}, \tag{6}$$

$$H_0 = 2m(\Psi_\downarrow^\dagger \Psi_\downarrow - \Psi_\uparrow^\dagger \Psi_\uparrow), \tag{7}$$

$$H_{int} = \sqrt{\frac{8}{N}} \Psi_\uparrow^\dagger \Psi_\downarrow \sum_{\mathbf{k}} \gamma_{\mathbf{k}} (u_{\mathbf{k}} \beta_{\mathbf{k}} + v_{\mathbf{k}} \alpha_{-\mathbf{k}}^\dagger) + \text{ h.c.}, \tag{8}$$

where N is the total number of lattice sites, and $u_{\mathbf{k}} = \sqrt{\frac{1}{2} + \frac{1}{\varepsilon_{\mathbf{k}}}}$, $v_{\mathbf{k}} = -\text{sign}(\gamma_{\mathbf{k}}) \sqrt{-\frac{1}{2} + \frac{1}{\varepsilon_{\mathbf{k}}}}$ are the parameters of the Bogoliubov transformation. Here we have assumed that the spins $\vec{S}_i, i = 2, .., 5$ belong to the B sub-lattice (spin down).

We define the Green's functions for the two fermion and spin-wave species: $G_\mu(t) = -i < T(\Psi_\mu(t) \Psi_\mu^\dagger(0)) >$, $\mu = \uparrow, \downarrow$, $\quad D(\mathbf{k}, t) = -i < T(\beta_{\mathbf{k}}(t) \beta_{\mathbf{k}}^\dagger(0)) >$ (and similarly for $\alpha_{\mathbf{k}}$). The unperturbed Green's functions ($H_{int} = 0$) are:

$$G_{\uparrow,\downarrow}(\omega) = \frac{1}{\omega \pm 2m + i\delta}, \quad D(\mathbf{k}, \omega) = \frac{1}{\omega - \epsilon_{\mathbf{k}} + i\delta}. \tag{9}$$

Next, the term H_{int} is treated in perturbation theory. The self-energy to one-loop order is given by the diagram in Fig.1a :

$$\Sigma_\uparrow(\varepsilon) = i \frac{8}{N} \sum_{\mathbf{k}} \gamma_{\mathbf{k}}^2 u_{\mathbf{k}}^2 \int D(\mathbf{k}, \varepsilon') G_\downarrow(\varepsilon - \varepsilon') \frac{d\varepsilon'}{2\pi} = \frac{8}{N} \sum_{\mathbf{k}} \frac{\gamma_{\mathbf{k}}^2 u_{\mathbf{k}}^2}{\varepsilon - 2m - \varepsilon_{\mathbf{k}}}. \tag{10}$$

Thus the spectral function of the $\Psi_\uparrow$ particles to this order is[11]:

$$A_\uparrow(\varepsilon) = -\frac{1}{\pi} \text{Im} G_\uparrow^{ret}(\varepsilon) = \delta(\varepsilon + 2m - \Sigma_\uparrow(\varepsilon)) \equiv Z \delta(\varepsilon - \varepsilon^*), \tag{11}$$

where ε^* is the solution of the equation:

$$\varepsilon^* + 2m - \Sigma_\uparrow(\varepsilon^*) = 0. \tag{12}$$

The renormalization factor Z is determined from (11):

$$Z = 1 + \frac{\partial \Sigma_\uparrow(\varepsilon^*)}{\partial \varepsilon}. \tag{13}$$

The ground state wave function of the Ψ particle - spin-wave system is then:

$$|G> = \sqrt{Z}\Psi^\dagger_\uparrow|0> + \sum_{\mathbf{k}} A_{\mathbf{k}} \Psi^\dagger_\downarrow \beta^\dagger_{\mathbf{k}}|0>, \tag{14}$$

where $|0>$ is the vacuum for the Ψ_μ and the spin-wave operators:

$$\Psi_\mu|0> = \alpha_{\mathbf{k}}|0> = \beta_{\mathbf{k}}|0> = 0. \tag{15}$$

From now on we will also adopt the short-hand notation:

$$|\mu> \equiv \Psi^\dagger_\mu|0>, \quad |\mu,\beta> \equiv \Psi^\dagger_\mu \beta^\dagger_{\mathbf{k}}|0>, \quad |\mu,\alpha> \equiv \Psi^\dagger_\mu \alpha^\dagger_{\mathbf{k}}|0>, \quad \mu = \uparrow, \downarrow . \tag{16}$$

The wave function (14) is a sum of coherent (first term) and incoherent part. In the coherent part, $\sqrt{Z}$ represents the probability amplitude of having the particle $\Psi_\uparrow$ (i.e. the spin $\vec{S}_1$ being up) in the ground state of H. The incoherent part comes from the admixture of intermediate states, each of them entering with probability amplitude

$$A_{\mathbf{k}} = \frac{<\downarrow,\beta|H_{int}|\uparrow>}{\varepsilon - 2m - \varepsilon_{\mathbf{k}}}. \tag{17}$$

It is easy to see that:

$$\sum_{\mathbf{k}} |A_{\mathbf{k}}|^2 = 1 - Z, \tag{18}$$

which reflects the normalization condition for $|G>$. Finally, the magnetization is:

$$< G|S^z_1|G> = \frac{1}{2}Z - \frac{1}{2}(1-Z) = 0.27. \tag{19}$$

The agreement between (19) and the spin-wave theory result ($m = 0.3$) is quite good. There are two ways to improve our calculation. First, two-loop (see Fig.2b), and higher order corrections can be included. Let us note that due to spin conservation there are no

vertex corrections to the self-energy (of the type, shown in Fig.2c). A similar phenomenon occurs in the $t-J$ model[12]. Second, we could define clusters of more than one spin as our "defect". Although the calculation accuracy is expected to improve by taking the above two points into account, the leading order result is quite reliable, and, for the problems considered in the next two sections, is in good agreement with numerical simulations.

III. FERROMAGNETIC BOND PROBLEM.

A. Theory.

Consider a ferromagnetic bond of strength K, connecting the sites 1 and 2:

$$H = H_J - K\vec{S_1}.\vec{S_2}, \tag{20}$$

where $K > 0$. The second term in (20) frustrates the LRO in the neighborhood of the defect and therefore leads to local suppression of the magnetization.

Following the idea, outlined in Sec.II, we separate the interactions into a part within the defect (i.e. between the spins $\vec{S_1}$ and $\vec{S_2}$) and a defect - spin-wave interaction. The Ising part of the latter is treated in mean-field approximation, whereas the transverse part (H_{int} below) is our perturbation:

$$H = H_{sw} + H_0 + H_{int}, \tag{21}$$

$$H_0 = -(K-1)\vec{S_1}.\vec{S_2} + 3m(S_2^z - S_1^z), \tag{22}$$

$$H_{int} = \sqrt{\frac{1}{2N}}\left\{S_2^+ \sum_{\mathbf{k}} \Gamma(\mathbf{k}) e^{ik_x}(u_{\mathbf{k}}\alpha_{\mathbf{k}}^\dagger + v_{\mathbf{k}}\beta_{-\mathbf{k}}) + S_1^+ \sum_{\mathbf{k}} \Gamma(\mathbf{k})(u_{\mathbf{k}}\beta_{\mathbf{k}} + v_{\mathbf{k}}\alpha_{-\mathbf{k}}^\dagger) + \text{h.c.}\right\}, \tag{23}$$

where

$$\Gamma(\mathbf{k}) = 2\cos(k_y) + \exp(ik_x), \tag{24}$$

and H_{sw} is given by (3). In (22) and (23) it is assumed that $\vec{S_1}$ belongs to sub-lattice A (spin up) and $\vec{S_2}$ - to sub-lattice B.

We introduce a fermion representation for the spins $\vec{S}_1$ and $\vec{S}_2$, similarly to (5), and call the corresponding fermions $\Psi_{\uparrow,\downarrow}$ and $\Phi_{\uparrow,\downarrow}$, respectively. Thus (22) and (23) should be thought of as expressed in terms of these fermions. In order to diagonalize H_0 it is convenient to define the two-particle matrix Green's function $\hat{G}_{\mu\nu}$:

$$\hat{G}_{\mu\nu}(t) = -i \begin{pmatrix} < T(\Psi_\uparrow(t)\Phi_\downarrow(t)\Psi_\uparrow^\dagger\Phi_\downarrow^\dagger) > & < T(\Psi_\uparrow(t)\Phi_\downarrow(t)\Psi_\downarrow^\dagger\Phi_\uparrow^\dagger) > \\ < T(\Psi_\downarrow(t)\Phi_\uparrow(t)\Psi_\uparrow^\dagger\Phi_\downarrow^\dagger) > & < T(\Psi_\downarrow(t)\Phi_\uparrow(t)\Psi_\downarrow^\dagger\Phi_\uparrow^\dagger) > \end{pmatrix}. \tag{25}$$

As (25) suggests, the diagonal elements (11 and 22) correspond to the two-particle states $|1>\equiv|\uparrow\downarrow>$ and $|2>\equiv|\downarrow\uparrow>$, respectively, where the first arrow represents the spin $\vec{S}_1$ and the second one - the spin $\vec{S}_2$. The off-diagonal components represent transitions between these two states. For future purposes it is convenient to define also the states: $|3>\equiv|\uparrow\uparrow>$ and $|4>\equiv|\downarrow\downarrow>$. The unperturbed Green's functions (corresponding to H_0) are:

$$G_{11,22}(\omega) = \frac{1}{\omega - (K-1)/4 \pm 3m + i\delta}, \quad G_{12}(\omega) = G_{21}(\omega) = \frac{1}{\omega + (K-1)/2 + i\delta}. \tag{26}$$

Next, we evaluate the self-energies to lowest order in perturbation theory with respect to H_{int}. It is, in fact, more convenient to use the Releigh-Schröedinger perturbation theory, rather than Feynman's diagrammatic technique. Using notations, similar to (16), the expression for Σ_{11} is:

$$\Sigma_{11}(\varepsilon) = \sum_{\mathbf{k}} \frac{|<3,\alpha|H_{int}|1>|^2}{\varepsilon + (K-1)/4 - \varepsilon_{\mathbf{k}}} + \frac{|<4,\beta|H_{int}|1>|^2}{\varepsilon + (K-1)/4 - \varepsilon_{\mathbf{k}}}. \tag{27}$$

Here by H_{int} we mean the interaction Hamiltonian at fixed wave vector, i.e. (23) without the $\mathbf{k}$ summation. Evaluating (27), we get:

$$\Sigma_{11}(\varepsilon) = \frac{1}{N}\sum_{\mathbf{k}} \frac{|\Gamma(\mathbf{k})|^2 u_{\mathbf{k}}^2}{\varepsilon + (K-1)/4 - \varepsilon_{\mathbf{k}}}. \tag{28}$$

Similar calculations for the other two Green's functions give:

$$\Sigma_{22}(\varepsilon) = \frac{1}{N}\sum_{\mathbf{k}} \frac{|\Gamma(\mathbf{k})|^2 v_{\mathbf{k}}^2}{\varepsilon + (K-1)/4 - \varepsilon_{\mathbf{k}}}, \quad \Sigma_{12}(\varepsilon) = \frac{1}{N}\sum_{\mathbf{k}} \frac{\mathrm{Re}\left[\Gamma^2(\mathbf{k})e^{ik_x}\right] u_{\mathbf{k}} v_{\mathbf{k}}}{\varepsilon + (K-1)/4 - \varepsilon_{\mathbf{k}}}. \tag{29}$$

This is the one-loop result which is sufficient for our purposes. Let us mention that higher loop orders of perturbation theory for $\hat{G}_{\mu\nu}$ are more complicated than those for the one-particle propagator of Sec.II, because vertex corrections are allowed.

In order to evaluate various correlation functions, we proceed similarly to the calculation of the previous section. Since the Hamiltonian mixes the fermionic states $|1>$ and $|2>$, the equation for the effective energy level ε^*, corresponding to (12) now has the form:

$$\begin{vmatrix} \varepsilon^* - (K-1)/4 + 3m - \Sigma_{11}(\varepsilon^*) & -(K-1)/2 + \Sigma_{12}(\varepsilon^*) \\ -(K-1)/2 + \Sigma_{12}(\varepsilon^*) & \varepsilon^* - (K-1)/4 - 3m - \Sigma_{22}(\varepsilon^*) \end{vmatrix} = 0. \tag{30}$$

The correct normalized eigenstate is of the form $|12>= \mu_1|1> +\mu_2|2>$, where (μ_1, μ_2) is an eigenvector of the matrix in (30), and $\mu_1^2 + \mu_2^2 = 1$.

The ground state wave function can be written as:

$$|G>= \sqrt{Z}|12> + \text{incoherent part}, \tag{31}$$

where the incoherent part represents the contribution of the intermediate states $|3>$ and $|4>$. The normalization factor Z is defined as:

$$Z = 1 + \frac{\partial \tilde{\Sigma}(\varepsilon^*)}{\partial \varepsilon}, \tag{32}$$

where the self energy $\tilde{\Sigma}$:

$$\tilde{\Sigma}(\varepsilon) = \mu_1^2 \Sigma_{11}(\varepsilon) + \mu_2^2 \Sigma_{22}(\varepsilon) + 2\mu_1\mu_2\Sigma_{12}(\varepsilon). \tag{33}$$

The average of any spin operator $\hat{O}$ in the state $|G>$ is:

$$\begin{aligned} < G|\hat{O}|G> &= < 12|\hat{O}|12> Z + \sum_{i=3\alpha,4\beta} \sum_{\mathbf{k}} \frac{|<i|H_{int}|12>|^2}{[\varepsilon + (K-1)/4 - \varepsilon_{\mathbf{k}}]^2} < i|\hat{O}|i> \\ &= < 12|\hat{O}|12> Z + \frac{1-Z}{2} \sum_{i=3,4} < i|\hat{O}|i> . \end{aligned} \tag{34}$$

Using the above formula, we get for the magnetization and the longitudinal and transverse spin-spin correlation functions:

$$M \equiv < S_1^z >= \frac{\mu_1^2 - \mu_2^2}{2} Z, \tag{35}$$

$$C_L(1,2) \equiv < S_1^z S_2^z >= -\frac{1}{4} - \frac{1}{2}(Z-1), \tag{36}$$

$$C_T(1,2) \equiv \frac{1}{2} < S_1^+ S_2^- + \text{h.c.} >= \mu_1\mu_2 Z. \tag{37}$$

The numerical evaluation of the sums (28) and (29) and the solution of (30) are straightforward. The correlators are then computed by using Eqs.(32,33,35-37).

B. Exact diagonalization studies.

To estimate the accuracy of our analytic approach we have obtained numerical results by exact diagonalization of small clusters. Instead of using periodic boundary conditions, we have applied a staggered magnetic field in the z direction to spins on the boundary of the cluster. This breaks the sublattice symmetry and allows us to compute single-spin averages as well as to distinguish between longitudinal and transverse correlations.

This procedure of course also breaks the translational invariance of the cluster and will, in general, lead to increased finite size effects and slow convergence to the bulk limit. We have chosen a cluster of N = 18 sites and a boundary field to give $< S^z >= 0.3$ on the boundary spins. Extremely good qualitative agreement was obtained with the analytical results, and tuning of the field would achieve even better agreement. This however is not warranted without, at the same time, a systematic extrapolation of the cluster results to the thermodynamic limit.

C. Results.

The results obtained by the Green's function method as well as the exact diagonalization results are summarized in Figures 2 and 3.

Figure 2 plots the local magnetization M and the total spin-spin correlation function across the FMB $C(1,2) \equiv < \vec{S}_1.\vec{S}_2 >= C_L(1,2) + C_T(1,2)$ as a function of frustration K. We have also calculated M by using LSWA, essentially following Lee and Schlottmann[4]. By treating K as a perturbation one can, in fact, exactly solve the Dyson equation for the spin-wave Green's function[4]. The LSWA result shows that the magnetization vanishes around $K = 1.9$ and an instability occurs at $K = 2$, which is the point when a local triplet formation is expected to occur classically.

Our result (35) shows qualitatively different behavior. Up to $K = 1$ the two curves follow each other closely, both predicting a slight increase of M at that value (corresponding

to a missing bond). A similar suppression of quantum fluctuations was observed in the case of a missing site[13]. However, beyond $K = 1$ we predict that the local magnetization decreases slowly and stays non-zero even for large K. On the other hand, the correlator $C(1,2)$ changes sign and becomes ferromagnetic at around $K = 2.1$. As shown in Figure 3, it is, in fact, the transverse part of the correlator that changes sign, while the Ising part has antiferromagnetic sign for all K. With increasing K the transverse part increases and the Ising one decreases (in magnitude), but remains non-zero, which is consistent with a finite magnetization.

The exact diagonalization results agree qualitatively well with those obtained by the Green's function method.

We would like to stress that, as our results show, the range of validity of the LSWA is limited to small frustration only ($K < 1$). Beyond this point the number of generated spin waves is large and the interactions between them become important. The vanishing of the magnetization in LSWA is thus an artifact of the approximation. Our treatment, on the other hand, is applicable far beyond $K = 1$.

IV. IMPURITY SPIN PROBLEM.

In this section we consider local frustration due to an additional quantum spin $\vec{\sigma}$ ($\sigma = 1/2$), coupled symmetrically to the two sub-lattices:

$$H = H_J + L\vec{\sigma}.(\vec{S_1} + \vec{S_2}) - \vec{S_1}.\vec{S_2}. \tag{38}$$

For either sign of the coupling L, the second term in (38) frustrates the spins $\vec{S_1}$ and $\vec{S_2}$. It is also assumed that the impurity spin effectively removes the superexchange between them[8].

Similarly to the approach used in Sec.III, first we diagonalize the second term in (38) exactly, and then treat the interaction of $\vec{S_1}$ and $\vec{S_2}$ with the AFM background (spin waves) perturbatively. Thus we have:

$$H = H_{sw} + H_0 + H_{int}, \tag{39}$$

where

$$H_0 = L\vec{\sigma}.(\vec{S_1} + \vec{S_2}) + 3m(S_2^z - S_1^z), \tag{40}$$

and H_{sw} and H_{int} are given by (3) and (23) respectively. We have assumed, as in the derivation of (23), that $\vec{S_1} \in$ (sub-lattice A), $\vec{S_2} \in$ (sub-lattice B).

In order to diagonalize H_0, define the bare states (the arrows represent, from left to right, the z components of $\vec{S_1}$, $\vec{\sigma}$ and $\vec{S_2}$):

$$|1>=|\uparrow\uparrow\downarrow>, |2>=|\downarrow\uparrow\uparrow>, |3>=|\uparrow\downarrow\uparrow>,\ S_{tot}^z = 1/2, \tag{41}$$

$$|4>=|\uparrow\downarrow\downarrow>, |5>=|\downarrow\downarrow\uparrow>, |6>=|\downarrow\uparrow\downarrow>, S_{tot}^z = -1/2, \tag{42}$$

$$|up>=|\uparrow\uparrow\uparrow>,\ S_{tot}^z = 3/2. \tag{43}$$

Observe that $S_{tot}^z = \sum_i S_i^z + \sigma^z$ is conserved and thus each sector can be dealt with separately. Diagonalizing H_0 in the sectors $S_{tot}^z = \pm 1/2$:

$$\det(< i|H_0|j > -\varepsilon\delta_{ij}) = 0 \tag{44}$$

we get the eigenenergies ε_i which correspond to the eigenvectors:

$$|i+>=\sum_{j=1}^{3} a_{ij}|j>, S_{tot}^z = 1/2, \tag{45}$$

$$|i->=\sum_{j=4}^{6} a_{ij}|j>, S_{tot}^z = -1/2. \tag{46}$$

Both states are assumed to be normalized. The above two sectors have the lowest energy (compared to $S_{tot}^z = \pm 3/2$) and are degenerate. For definiteness we choose, for example $S_{tot}^z = 1/2$. It will be proven below, both analytically and numerically that the ground state of H stays in this sector for any L even after H_{int} is taken into account.

In order to develop a perturbation theory in H_{int} it is convenient to introduce Green's functions. Since there are three states of three particles, we have to consider a 3×3 matrix three-particle Green's function $\hat{G}_{ij}, i, j = 1, 2, 3$. The poles of $\hat{G}_{ij}$ are the matrix elements $< i|H_0|j >$. In order to define $\hat{G}_{ij}$ let us introduce a fermionic operator representation for

the three spins, analogously to (5). The fermions representing $\vec{S}_1$, $\vec{S}_2$ and $\vec{\sigma}$ are Ψ_μ, Φ_μ and Θ_μ, respectively, $\mu = \uparrow, \downarrow$. The Hamiltonian now should be thought of as expressed in terms of these operators. Then, for example $\hat{G}_{11}$ is defined as:

$$\hat{G}_{11}(t) = -i < T(\Psi_\uparrow(t)\Theta_\uparrow(t)\Phi_\downarrow(t)\Psi^\dagger_\uparrow\Theta^\dagger_\uparrow\Phi^\dagger_\downarrow) >, \tag{47}$$

and similarly for all the others. The unperturbed Green's functions are:

$$\hat{G}^{-1}_{ij}(\omega) = \omega - < i|H_0|j > + i\delta, \quad i,j = 1,2,3. \tag{48}$$

To lowest order of perturbation theory with respect to H_{int}, the self-energies, corresponding to $\hat{G}_{ij}$ are calculated as:

$$\Sigma_{ij}(\varepsilon) = \sum_{l=1}^{3}\sum_{\mathbf{k}} \frac{< i + |H_{int}|l-, \beta >< l-, \beta|H_{int}|j+ >}{\varepsilon - \varepsilon_l - \varepsilon_{\mathbf{k}}} + \sum_{\mathbf{k}} \frac{< i + |H_{int}|up, \alpha >< up, \alpha|H_{int}|j+ >}{\varepsilon - \varepsilon_{up} - \varepsilon_{\mathbf{k}}}, \tag{49}$$

where $\varepsilon_{up} = L/2$ is the energy, corresponding to the state $|up>$ (43).

Then the equation for the effective energy level ε^* (compare with (30)) is:

$$\det((\varepsilon_i - \varepsilon^*)\delta_{ij} + \Sigma_{ij}(\varepsilon^*)) = 0. \tag{50}$$

The correct three-particle $S^z_{tot} = 1/2$ eigenstate is given by:

$$|123 >= \sum_{i=1}^{3} \mu_i |i+> . \tag{51}$$

Here μ_i are the normalized eigenvectors of the matrix in (50). The three-particle - spin-wave ground state to lowest order is, similarly to (31):

$$|G >= \sqrt{Z}|123 > + \text{incoherent part}. \tag{52}$$

The normalization factor Z is defined as:

$$Z = 1 + \sum_{i,j=1}^{3} \mu_i\mu_j \frac{\partial\Sigma_{ij}(\varepsilon^*)}{\partial\varepsilon}. \tag{53}$$

The incoherent part is a mixture of the intermediate states $|i-,\beta>$ and $|up,\alpha>$ with appropriate weights, which are too lengthy to write down explicitly.

Finally, the average of any combination of spin operators $\hat{O}$ in this ground state can be easily calculated:

$$< G|\hat{O}|G >=< 123|\hat{O}|123 > Z + \sum_{\mathbf{k}} \frac{|< up,\alpha|H_{int}|123 >|^2}{(\varepsilon - \varepsilon_{up} - \varepsilon_{\mathbf{k}})^2} < up|\hat{O}|up > + \sum_{l,m=1}^{3} \sum_{\mathbf{k}} \frac{< 123|H_{int}|m-,\beta >< l-,\beta|H_{int}|123 >}{(\varepsilon - \varepsilon_m - \varepsilon_{\mathbf{k}})(\varepsilon - \varepsilon_l - \varepsilon_{\mathbf{k}})} < m-|\hat{O}|l- > . \quad (54)$$

Using (54) we have calculated the spin-spin correlation functions for $\vec{S}_{1,2}$ and $\vec{\sigma}$, as well as the appropriate magnetizations. The following notations are adopted:

$$C(\sigma,i) \equiv < \vec{\sigma}.\vec{S}_i >, i = 1,2, \quad C(1,2) \equiv < \vec{S}_1.\vec{S}_2 >, \quad (55)$$

$$M(\sigma) \equiv < \sigma^z >, \; M(i) \equiv < S_i^z >, i = 1,2 \quad (56)$$

We have also performed numerical simulations, based on exact diagonalization on small clusters with typical size $N = 18+1$. The numerical procedure is similar to the one outlined in Sec.IIIB. All our results are summarized in Figures 4 and 5. We have checked with both methods that the ground state is in the sector $S^z_{tot} = 1/2$ for all L and thus no level crossing occurs.

For ferromagnetic value of the coupling, $L < 0$, all correlations become ferromagnetic for sufficiently large $|L|$(Fig.4.). However, this is not accompanied by a change in the ground state, since all the three spins have a non-zero magnetization (Fig.5.). This was already pointed out by Oitmaa, Betts, and Aydin[8]. The situation is rather similar to the case of a FMB in an AFM background, studied in the previous section.

For antiferromagnetic coupling, $L > 0$, there is a local ground state phase transition at $L \approx 2.3$, when the spins $\vec{S}_2$ and $\vec{\sigma}$ change the direction of their magnetization. Naturally, the magnetization of $\vec{S}_1$ increases at this point, since it is no longer frustrated. This local change in the ground state was observed numerically by Oitmaa, Betts, and Aydin[8]. However,

they found a discontinuity in all correlation functions as well as the magnetizations at the transition point, which was attributed to level crossing. We, on the other hand, observe a continuous transition. It is quite possible that the discontinuity is due to a finite size effect.

V. SUMMARY AND CONCLUSIONS.

In summary, we have developed an analytic technique which allowed as to study the effect of locally frustrating perturbations (static spin defects) in 2D quantum antiferromagnets for any strength of the coupling. Such defects are of relevance to the physical system of oxygen holes in the CuO planes of the high-T_c cuprates at low doping. All analytic results are in good agreement with numerical simulations, based on exact diagonalization on small clusters.

For an isolated ferromagnetic bond we found that the local magnetization does not vanish even for strong frustration. Our result suggests, that the previous calculations using LSWA[4,5] lead to qualitatively wrong behavior. The region of validity of LSWA is thus restricted to small frustration only.

We also studied frustration due to a quantum impurity spin coupled symmetrically to the two sub-lattices. It was found that for a ferromagnetic sign of the coupling there is no change in the ground state, similarly to the case of a FMB. For an antiferromagnetic interaction between the impurity and its neighbors we report a local change in the ground state.

The technique presented in this paper is not limited to the study of the above problems. It can be applied to any spin systems where LRO is suppressed locally due to additional interactions and represents a nice alternative to LSWA for strong interactions.

ACKNOWLEDGMENTS

The financial support of the Australian Research Council is gratefully acknowledged.

[1] For a review, see, E. Manousakis, Rev. Mod. Phys. **63**, 1 (1991).

[2] See, e.g., E. Dagotto, Rev. Mod. Phys. **66**, 763 (1994).

[3] A. Aharony, R. J. Birgineau, A. Coniglio, M. A. Kastner, and H. E. Stanley, Phys. Rev. Lett. **60**, 1330 (1988).

[4] K. Lee and P. Schlottmann, Phys. Rev. B **42**, 4226 (1990); S. Haas, D. Duffy, and P. Schlottmann, Phys. Rev. B **46**, 3135 (1992).

[5] D. N. Aristov and S. V. Maleev, Z. Phys. B **81**, 433 (1990).

[6] I. Ya. Korenblit, Phys. Rev. B **51**, 12551 (1995).

[7] J. R. Rodriguez, J. Bonca, and J. Ferrer, Phys. Rev. B **51**, 3616 (1995).

[8] J. Oitmaa and D. D. Betts, Physica A **177**, 509 (1991); J. Oitmaa, D. D. Betts, and M. Aydin, Phys. Rev. B **51**, 2896 (1995).

[9] D. G. Clarke, T. Giamarchi, and B. I. Shraiman, Phys. Rev. B **48**, 7070 (1993).

[10] V. Kotov, J. Oitmaa and O. Sushkov, J. Magn. Magn. Mat. **177-180**, (1998).

[11] G. D. Mahan, *Many Particle Physics*, Plenum, New York, 1990.

[12] O. P. Sushkov, Phys. Rev. B **49**, 1250 (1994).

[13] N. Bulut, D. Hone, D. J. Scalapino, and E. Y. Loh, Phys. Rev. Lett. **62**, 2192 (1989).

FIG. 1. Diagrams for the self-energy $\Sigma_{\uparrow}$: a) One-loop contribution. b),c) Examples of two-loop corrections. Solid lines represent fermionic Green's functions, while dashed lines are spin-wave propagators.

FIG. 2. Local magnetization M (solid line) and the correlation function $C(1,2)$ (long dashed line), calculated by using the Green's function method, as a function of the FMB strength K. The diamonds and squares are the corresponding exact diagonalization results. The short dashed line is the magnetization, calculated in LSWA.

FIG. 3. The transverse (solid line) and the longitudinal (dashed line) parts of the spin-spin correlation function across the FMB. The triangles and the circles are the corresponding exact diagonalization results.

FIG. 4. Correlations between the impurity spin and its neighbors, as defined in Eq.(55). The lines and the symbols represent, respectively, the analytical and the exact diagonalization results.

FIG. 5. The magnetization of the impurity (solid line) and the neighboring spins (dashed lines) as a function of the interaction L. The symbols represent the exact diagonalization results.

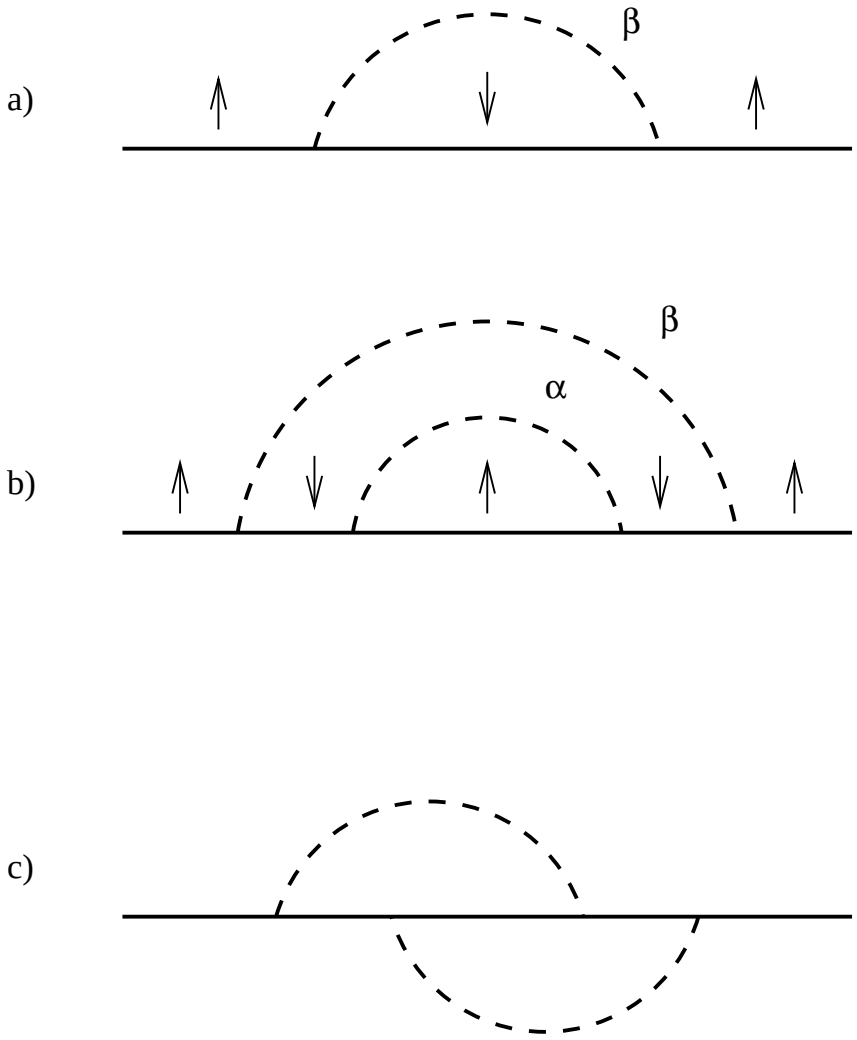

Fig.1.

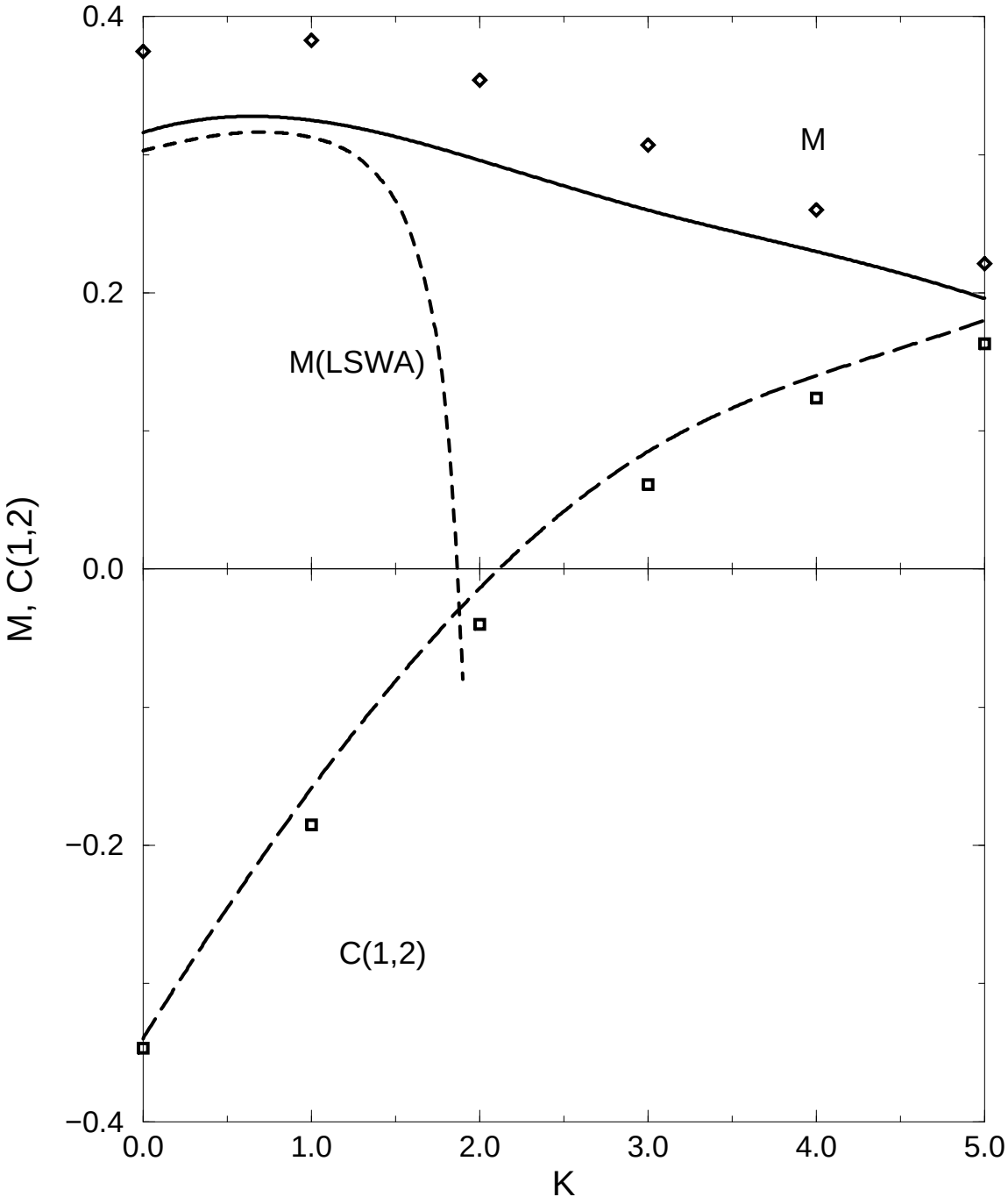

Fig.2.

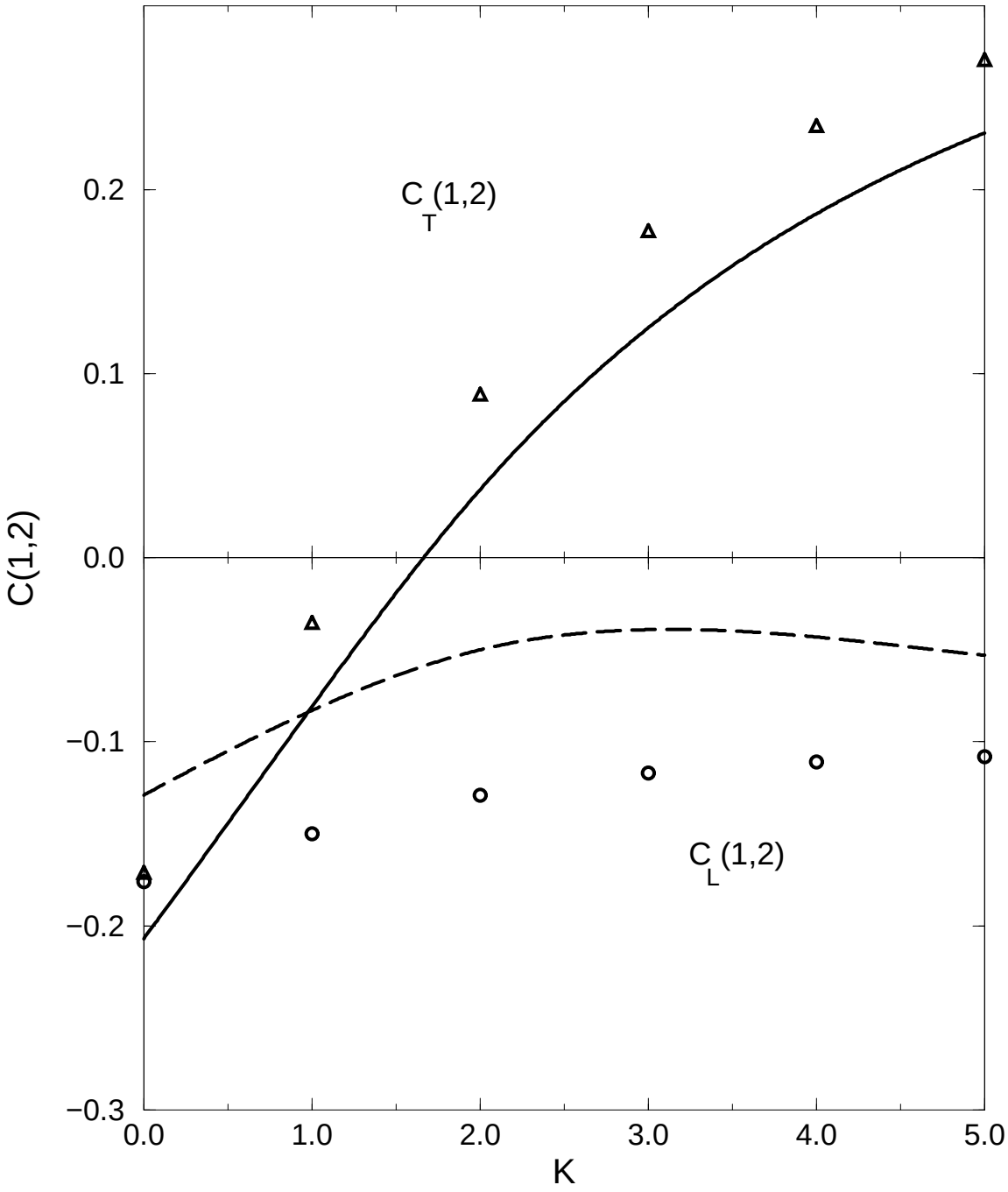

Fig.3.

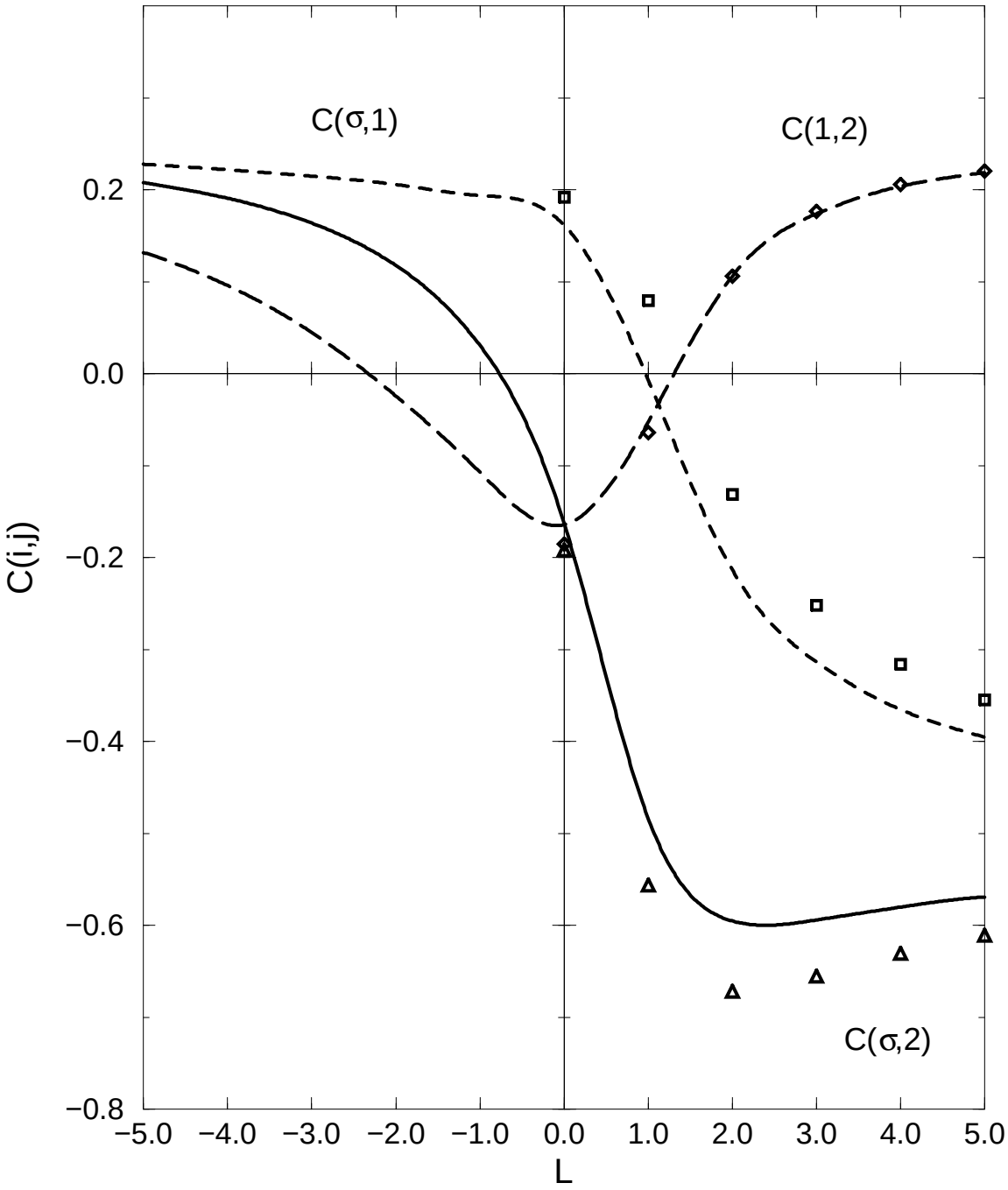

Fig.4.

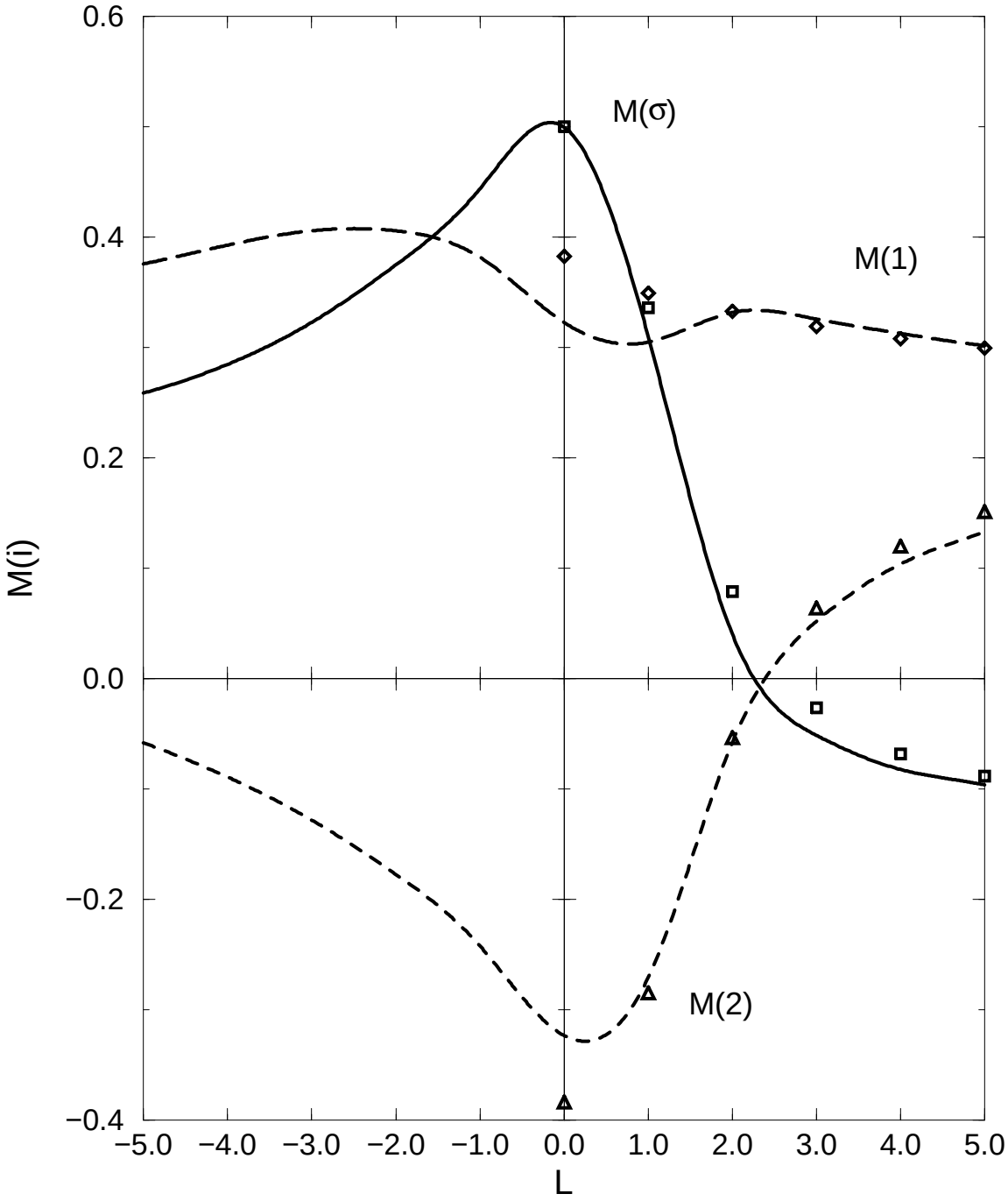

Fig.5.